PL-TR-95-2012

Typhoon Monitoring Using Passive Microwave Observations

Robert T. Merrill

University of Wisconsin-Madison
Space Science and Engineering Center (SSEC)
Cooperative Institute for Meteorological Satellite Studies (CIMSS)
1225 West Dayton Street
Madison, Wisconsin 53706

October 1994

Final Report
September 1992 - October 1994

19950327 068

"This technical report has been reviewed and is approved for publication."

GERALD W. FELDE
Contract Manager

DONALD A. CHISHOLM
Chief, Satellite Analysis and Weather
Prediction Branch
Atmospheric Sciences Division

ROBERT A. McCLATCHEY, Director
Atmospheric Sciences Division

REPORT DOCUMENTATION PAGE

1. AGENCY USE ONLY (Leave blank)	2. REPORT DATE October 1994	3. REPORT TYPE AND DATES COVERED Final (Sep 1992 – Oct 1994)

4. TITLE AND SUBTITLE	5. FUNDING NUMBERS
Typhoon Monitoring Using Passive Microwave Observations	PE 63707F PR 4026 TA 01 WU KJ
6. AUTHOR(S) Robert T. Merrill	MIPR FY7121-91-00003

7. PERFORMING ORGANIZATION NAME(S) AND ADDRESS(ES) University of Wisconsin-Madison Space Science & Engr Center (SSEC) Cooperative Inst for Meteorological Satellite Studies (CIMSS) 1225 W. Dayton St./Madison, WI 53706	8. PERFORMING ORGANIZATION REPORT NUMBER

9. SPONSORING/MONITORING AGENCY NAME(S) AND ADDRESS(ES) Phillips Laboratory 29 Randolph Road Hanscom AFB, MA 01731-3010 Contract Manager: Gerald W. Felde/GPAB	10. SPONSORING/MONITORING AGENCY REPORT NUMBER PL-TR-95-2012

11. SUPPLEMENTARY NOTES

12a. DISTRIBUTION/AVAILABILITY STATEMENT Approved for public release; distribution unlimited	12b. DISTRIBUTION CODE

13. ABSTRACT (Maximum 200 words)

Because tropical cyclones have deep warm cores they are amenable to monitoring using passive microwave radiometers in the 55 GHz (Oxygen) band. However, such radiometers currently have horizontal resolution of 100 km or more, which is significantly larger than the eye of most tropical cyclones. The warm anomaly directly observable in the brightness temperature distribution is therefore an underestimate of the actual warm anomaly strength. The subject of this contract is an algorithm to correct for this underestimate. Passive microwave observations are modeled as an interaction between the radiometer antenna pattern and an analytic function approximating the thermal structure of a tropical cyclone. Solution of the inverse of this model using a maximum likelihood method yields an estimate of the amplitude of the warm anomaly. Application of this technique to observations from two different radiometers (MSU and SSM/T) indicates that it is relatively successful at correcting for horizontal resolution differences. However, the warm anomalies so obtained are little better than the raw observations themselves as estimators of tropical cyclone intensity. Reasons for this are examined and some potential avenues of research are suggested.

14. SUBJECT TERMS tropical cyclones, remote sensing, passive microwave radiometry			15. NUMBER OF PAGES 28
			16. PRICE CODE

17. SECURITY CLASSIFICATION OF REPORT Unclassified	18. SECURITY CLASSIFICATION OF THIS PAGE Unclassified	19. SECURITY CLASSIFICATION OF ABSTRACT Unclassified	20. LIMITATION OF ABSTRACT SAR

Table of Contents

Acknowledgments

1.   Using This Report

The focus of this final report (Chapter 2) is on the scientific results of the work done in pursuit of the objectives stated in the Proposals for "Typhoon Monitoring Using Passive Microwave Observations." A software package along with a Users' Guide and Software Development and Maintenance Guide were developed as part of this project. Chapters 3 and 4 are overviews of these two Guides. Persons interested in obtaining the software and complete versions of the two Guides should contact the author.

2. Project Objectives and Results

2.1. Overview

This Chapter summarizes each of the stated objectives and intended results from the two proposals submitted for this program. Two of the main results are the Users' Guide and the Software Development and Maintenance Guide and are included by reference only in the final report. Many of the other results are covered implicitly in these two Guides and are cross-referenced here. Other results have been presented in detail in the refereed literature as cited.

2.2. Problem Summary

Proposal task: Establish theoretical relationship between passive microwave observations and tropical cyclone intensity

Tropical cyclone intensity monitoring from satellites has followed two paths, dictated by the types of satellite instruments available and the physical characteristics of the problem. Operational measures of tropical cyclone intensity are minimum sea level pressure (MSLP) and maximum sustained wind (MSW), nominally a 1-minute mean wind at a height of 10 m from the surface. Because tropical cyclones are generally in hydrostatic balance, the MSLP could theoretically be computed directly from the pressure at any height above the surface (a 'reference level') if the three-dimensional thermal structure were known.

The first satellite instruments, and still the most widely available types, measured reflected visible and emitted infrared radiation. These provide an excellent depiction of clouds but are useless for estimating vertical soundings of temperature in cloudy areas. It was quickly found that the patterns or degree of organization in the clouds was empirically related to the intensity of the storm. Dvorak (1975, 1984) classified these patterns for many tropical cyclones and developed a rule-based technique that is today in worldwide use.

The availability of passive microwave observations in the 55 GHz band made remote temperature estimates in cloudy atmospheres possible, and early experiments determined that the warm core of tropical cyclones was indeed evident in the data (see Velden 1989, Velden *et al.* 1991, and Merrill 1995 for an historical survey). Still, these radiometers have several limitations that made direct retrieval of the three-dimensional thermal structure of a tropical cyclone extremely difficult.

1) The long wavelengths of microwave radiation (relative to visible and infrared) and the engineering limitations on antenna sizes means that the horizontal resolution of passive microwave radiometers is relatively poor (100-200 km). This is significantly larger than the area covered by the strongest warm anomaly of a tropical cyclone (the eye), that has a scale of 10-100 km.

2) The relatively low power of microwave radiation means a relatively poor signal-to-noise ratio for passive microwave sounders.

Table 1. A summary of possible approaches to the problem of quantitative tropical cyclone intensity estimation from passive microwave observations. Within each category, models are listed in order of increasing scope of input data. References are given for those models that have actually been attempted.

Statistical models

Type	Input Data	Algorithm	Reference
S1	Upper-tropospheric channel	Regression Model (satellite and basin specific)	Velden (1989), Velden et al. (1991)
S2	Upper-tropospheric channel Other channels	Regression Model (satellite and basin-specific)	

Hybrid models

Type	Input Data	Stage 1 Algorithm	Intermediate Result	Input to Stage 2	Stage 2 Algorithm	Reference
H1	Upper-tropospheric channel	horizontal structure retrieval	B(x,y)	delB	Regression Model (basin specific)	Merrill (1995) and this Report
H2	Upper-tropospheric channel	horizontal structure retrieval	B(x,y)	delB, Lower-tropospheric channel	Regression Model (basin and satellite specific)	this Report
H3	Upper-tropospheric channel Other channels	sounding retrieval	T(p)	delT at 250 hPa	Regression Model (basin and satellite specific)	Velden (1989), Velden et al. (1991)

Type	Input Data	Stage 1 Algorithm	Intermediate Result	Stage 2 algorithm	Input to Stage 3	Stage 3 Algorithm
H4	Upper tropospheric channel Other channels	sounding retrieval	T(p) at each field of view	horizontal structure retrieval	satellite-independent upper-tropospheric T	Regression model (basin specific)

Physical model

Type	Input data	Stage 1 Algorithm	Intermediate Result/Input to stage 2	Stage 2 Algorithm	Intermediate Result	Stage 3 algorithm
P1	Upper tropospheric channel	horizontal structure retrieval	B(x,y) for upper tropospheric channel	sounding retrieval	T(p) at storm center	hydrostatic integration
	Other channels		Other channels			
P2			Upper-tropospheric channel Other channels	Three-dimensional retrieval	T(x,y,p)	hydrostatic integration
	Imager (window) channel(s), i.e. SSM/I	Precipitation Retrieval	Precipitation distribution			

3) Though generally unaffected by clouds when compared with infrared, microwave radiation is still somewhat attenuated by them, and precipitation-sized hydrometeors are extremely effective scatterers of microwaves. Microwave emissions from regions below the melting level, or in regions of active precipitation, are attenuated by scattering.

Because of the above limitations, it is impossible using 55 GHz data alone to retrieve the temperature structure with sufficient horizontal resolution to measure the peak warming at any altitude, and it is impossible to detect the warm anomaly below the melting level at all in most tropical cyclones. Still, the warm anomaly is at least detectable, and is known to be physically related to tropical cyclone intensity. In order to do so quantitatively, the effects of poor horizontal resolution and scattering must be accounted for somehow, either statistically or by direct correction for these effects via radiative transfer calculations. The differences in all tropical cyclone monitoring efforts to date differ mainly in which parts of the problem are solved physically and which are addressed statistically.

3

Table 1 summarizes the various approaches to solving this problem. Some are conceptual and others have been attempted. Estimating MSLP and to a somewhat lesser extent MSW is straightforward if the three-dimensional temperature structure T(x,y,p) is known. If T(x,y,p) cannot be determined, then a statistical method has to be used to estimate intensity from what can be estimated from the microwave data. The models are grouped according to the relative use of statistical and physical methods, and within each group, models are listed in order of increasing scope of the input data.

The purely statistical models make no attempt at converting observations (brightness temperatures) to atmospheric temperatures as an intermediate step. Intensity is estimated directly from the observations. The properties of the vertical weighting functions, beam-filling problems due to the large fields of view relative to the warm anomaly, scattering by precipitation, and inter-basin differences in tropical cyclone structure are all accounted for, at least in an implicit, mean sense, by the regression equations. This approach has two major limitations:

1) Separate sets of dependent data (*in situ* intensity measurements and microwave observations) must be available for each population (tropical cyclone basin and satellite type).

2) The greater the number of predictors and nonlinearity of the problem, the more carefully the form of the model must be chosen and its significance tested, particularly for small sample sizes.

The first limitation is sufficiently great to motivate at least a hybrid physical solution in an attempt to eliminate at least the differences between satellites so that estimates can be made from the newer satellites of the post-reconnaissance era. The pure statistical models cited have been simple enough that limitation 2 has not yet been an issue, although this would change if an attempt at building an S2 model with statistical precipitation correction, for example, were attempted.

The present model (H1 and H2; Merrill 1995) and those of Velden (1989) and Velden *et al.* (1991) are hybrids. These models attempt to solve a portion of the problem directly to produce an intermediate result that is a better statistical estimator of intensity than are observed brightness temperatures. They differ in their division of labor between physical and statistical solutions. H1 and H2 are the subject of this Report and Merrill (1995) and attempt to correct for the field of view size differences between satellites with a physical solution for a single upper-tropospheric channel. The techniques are able to produce consistent estimates of upper-tropospheric warm anomaly strengths from different satellites (see Section 2.5) but their usefulness as intensity estimators is strongly dependent upon accurate estimates of eye size and correction for precipitation scattering effects (see Section 2.6). H2 makes a crude statistical correction for the latter by introducing a lower-tropospheric brightness temperature into the statistical component. This improves the results but also re-introduces a satellite-dependent component, the very limitation the horizontal structure retrieval approach was intended to avoid. The H3 model uses the most data (all channels), contains some correction for precipitation effects, and produces the best estimates but cannot eliminate inter-satellite differences due to field of view sizes and so is limited to use with MSU data.

A possible improvement is hybrid model H4. In this model, H3 would be used as the first stage algorithm to produce upper tropospheric temperatures that have been corrected in part for precipitation scattering by the sounding retrieval algorithms for SSM/T or MSU. These upper-tropospheric temperatures would then serve as inputs to the horizontal retrieval, as is done with upper-tropospheric brightness temperatures in H1 and H2. The intended result is an upper-tropospheric warm anomaly strength, including corrections for both field of view differences and precipitation effects, that could serve as a satellite-independent estimator of intensity via a statistical model. The statistical model would be fitted

to MSU only because of *in situ* data restrictions. The success of stage 2 could be evaluated using match pair analysis of its outputs as was done with H1 output (Section 2.5).

The only pure physical solution attempted (P1) was a failure (see Section 2.10 topic "Eye sounding feasibility study"). The 'ultimate' physical solution (P2) would involve a full three-dimensional retrieval of temperature from brightness temperatures using explicit correction for precipitation effects, either from a previous precipitation retrieval from microwave window channel data (SSM/I) or as part of a simultaneous solution.

2.3. Statistical Estimates Based on Soundings Retrieved from MSU

Proposal task: Build, evaluate, and publish a statistical model based on sounding retrievals

The simplest method for monitoring tropical cyclone intensity from passive microwave observations is to form a statistical relationship between some readily obtainable index of warm anomaly strength and *in situ* estimates of intensity. This approach was used by Velden *et al.* (1991) for MSU. Warm anomaly strengths were estimated both from channel 3 (54.96 GHz) brightness temperatures (B3) and from 250 hPa temperatures (T250) retrieved from all four MSU channels using the TOVS (TIROS Operational Vertical Sounder consisting of HIRS -- High-resolution InfraRed Sounder and MSU -- Microwave Sounding Unit) retrieval package on the SSEC McIDAS. The warm anomaly (dB3 or dT250) was determined by subtracting an environmental value of B3 or T250 from the value at the storm center; and the environmental value was computed by averaging 10 values just outside the storm's cirrus canopy as seen in HIRS window channel data. The *in situ* data were provided by reconnaissance aircraft -- either maximum sustained winds (MSW) or minimum sea level pressures (MSLP). The MSLP values were then used to compute pressure reductions (dP) by subtracting them from environmental pressures estimated from surface analyses.

A set of 82 cases of dB3, dT250, MSW, and dP was assembled and subjected to thorough statistical analysis and the relationships

$$dP = 1.79 + 13.28 * dT250 - 0.42 * (dT250)^2, \quad SEE = 13.7 \text{ hPa}$$

$$MSW = 30.7 + 15.32 * dT250 - 0.63 * (dT250)^2, \quad SEE = 16.7 \text{ ms}^{-1}$$

(1)

obtained. Relationships based on dT250 explained 73% of the variance in dP and 65% of the variance in MSW, while those using dB3 (not shown) explained 65% and 58%, respectively, showing that the vertical sounding retrieval process, even near the storm center where scattering due to precipitation overwhelms MSU channels 1 and 2, adds useful information to the process.

Velden *et al.* (1991) also compared the linear versions of the above equations with those derived for Atlantic hurricanes (Velden 1989) and concluded that the relationships were not interchangeable, probably because of the smaller mean horizontal scale of the warm anomaly in Atlantic storms than in western North Pacific ones. It was also concluded that the MSU relationships for either basin could not be used with SSM/T-derived data because of the different sizes of the antenna patterns. These issues, combined with the lack of simultaneous SSM/T archived data and reconnaissance in western North Pacific tropical cyclones, motivated the research on the physical retrieval of the horizontal structure of a warm anomaly supported by these projects.

5

The above relationships have been rederived for a 79-case subset of the Velden *et al.* (1991) sample using warm anomaly strengths obtained from the horizontal structure retrieval algorithm. These results are presented and discussed in Section 2.6.

2.4. Prototype Algorithm

Proposal task: Develop a prototype algorithm for retrieving the warm anomaly structure and amplitude from MSU or SSM/T using real data.

Proposal task: Conduct an error analysis using simulated MSU and SSM/T observations

The algorithm has been implemented as a pair of MS-DOS applications described in detail in Chapter 3, "Users' Guide," and Chapter 4, "Software Development and Maintenance Guide." The relative ability of the algorithm to retrieve warm anomaly strengths using MSU and SSM/T data has been examined using both simulation studies, published as Merrill (1995), and empirical studies, summarized in Sections 2.5 and 2.6.

2.5. Comparisons of Warm Anomaly Strengths Retrieved from MSU and SSM/T

Summary:

1) The retrieval algorithm reduces the scatter between SSM/T and MSU warm anomaly estimates as expected.

2) The retrieval algorithm amplifies the warm anomaly signal for both SSM/T and MSU as expected. The amplification is greater for SSM/T as expected because its field of view is larger.

3) Warm anomaly estimates from raw SSM/T data are slightly stronger than those from MSU. This is not expected. Possible causes are a greater susceptibility of MSU to scattering by hydrometeors and deficiencies in SSM/T limb correction.

4) Because of 2) and 3), retrieved warm anomaly strengths from SSM/T are systematically warmer than those from MSU. Before comparing warm anomaly estimates from the two sensors, the SSM/T estimates should be corrected. Linear regression (minimum variance) and maximum likelihood relationships are provided.

The purpose of the horizontal retrieval algorithm is to eliminate the effects of antenna pattern size and viewing geometry from warm anomaly estimates. Nearly simultaneous views of a storm by MSU and SSM/T should produce nearly identical warm anomaly estimates, regardless of whether the storm was centered within a field of view, bracketed between several, or located on in the center of the data sector or near the edge. Given that the SSM/T antenna pattern is larger than MSU, SSM/T warm anomalies computed directly from the limb-corrected data (brightness temperatures) should be consistently weaker for SSM/T and positively correlated with MSU estimates, but with moderate scatter due to viewing geometry variations. After retrieval, the SSM/T and MSU warm anomaly estimates should all lie along a straight line through the origin and having slope 1.

In order to test the above expectations, data were collected in near real time for selected tropical cyclones worldwide from August 1993 through January 1994. From these data, instances of SSM/T and MSU overpasses within 6 h of each other were selected as match pairs. Each was carefully reviewed and
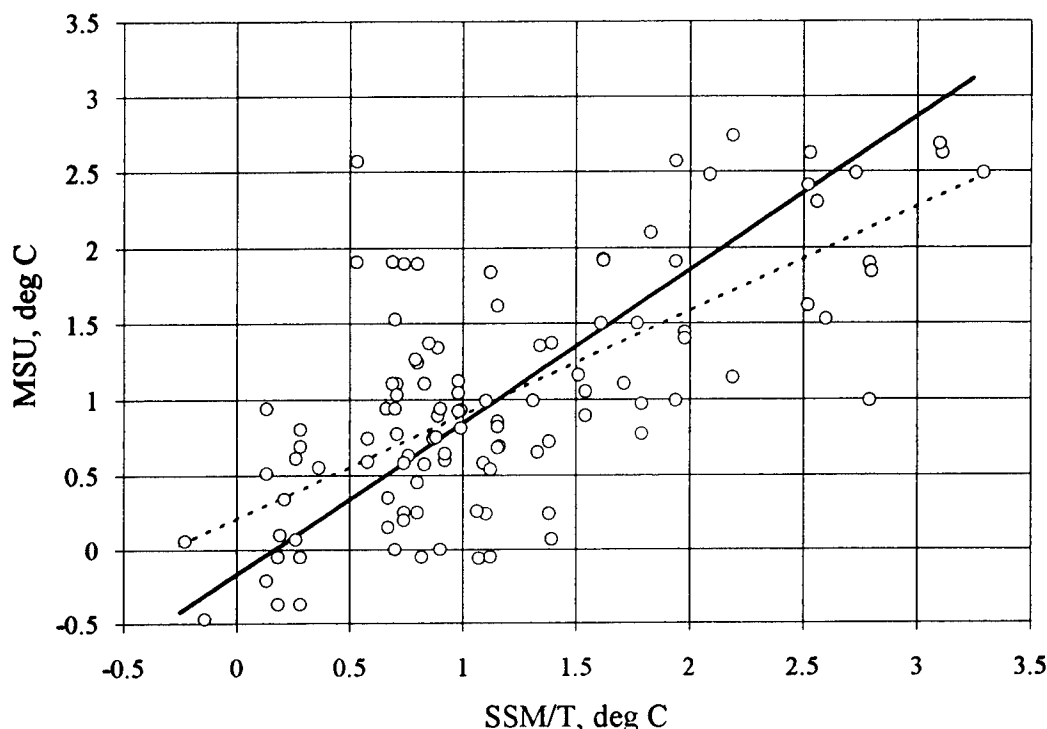
Fig. 1. The relationship between raw warm anomaly strengths computed from nearly simultaneous (within 6 h) observations in SSM/T channel 4 and MSU channel 3. Two linear fits to the data are shown. The maximum likelihood line (solid) is MSU = -0.17 + 1.01*SSM/T and the regression line is MSU = 0.21 + 0.69*SSM/T and explains 47% of the variance in the raw MSU warm anomalies.

those having large quantities of missing data or exceptionally poor viewing geometry were eliminated and a set of 109 pairs produced. The results of the match pair tests are shown in Figs. 1 and 2 and Table 2.

Fig. 1 shows the relationship between raw warm anomaly strengths from SSM/T and MSU for each match pair. The raw warm anomaly is computed by taking the brightness temperature nearest the storm center and subtracting from it the average of four brightness temperatures in the near environment at a radius of 500-750 km. Two forms of linear relationship are shown. Linear regression minimizes the squared deviations of MSU warm anomaly strength only from the fitted line, while maximum likelihood estimation minimizes the squared deviations of both MSU and SSM/T warm anomaly from the fitted line. In other words, the 'distances' from scatter plot points to the line are computed parallel to the ordinate for regression and normal to the line itself for maximum likelihood with the result that the maximum likelihood relationship more nearly resembles an 'eyeball' fit, especially for a data set like this where the variances in the two quantities are roughly similar. Fig. 2 is identical to Fig. 1 except it was prepared for warm anomaly strengths produced by the horizontal structure retrieval algorithm. These particular results were obtained using a specified observation noise of 1.0 °K. This value was tentatively chosen based on the known radiometer noise in the 0.5 °K range and increased to account for errors in the forward model due to warm anomaly structure variability in patterns that cannot be represented by the retrieved structure. The value was then confirmed by an experiment using values of 0.5, 1.0, 2.0, 4.0, or 8.0 °K, and at 1.0 °K the

7
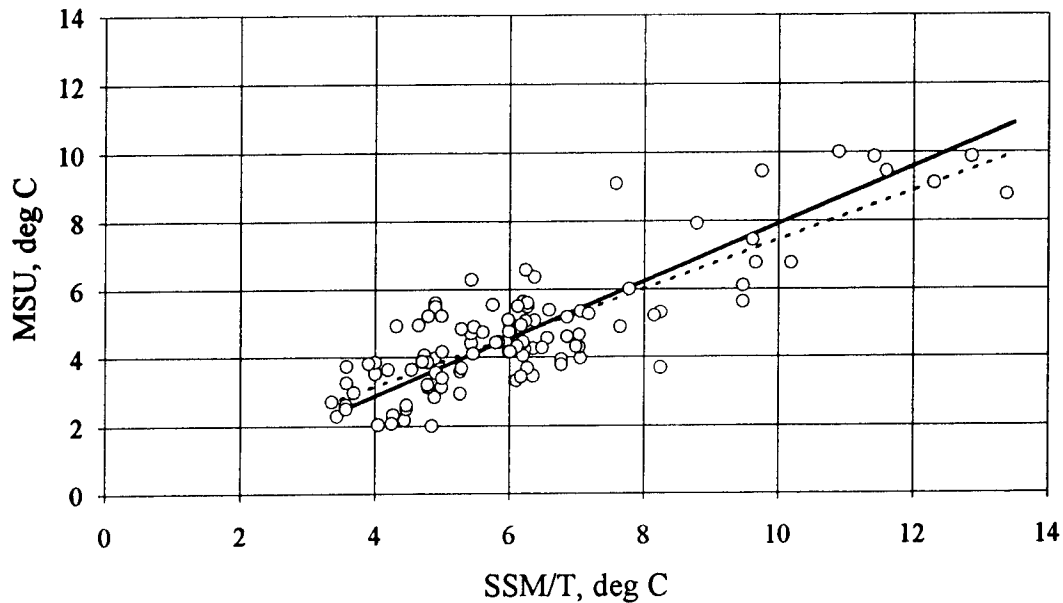
Fig. 2. As Fig. 1 except for retrieved warm anomaly strengths computed using a specified observation noise of 1.0 °K. The maximum likelihood fit (solid) is MSU = -0.49 + 0.84*SSM/T and the regression fit (dashed) is MSU = 0.26 + 0.72*SSM/T and explains 69% of the variance in the retrieved MSU warm anomaly strengths.

percent variance explained by a linear relationship between SSM/T and MSU estimates reached a maximum of 69%.

Fig. 1 and Table 2 indicate that the data themselves have some unexpected characteristics. Because of its larger antenna pattern, it is expected that the SSM/T raw warm anomalies would be weaker than those from MSU, but the range, mean, and median information show that the SSM/T warm anomalies are actually slightly stronger. Two possible reasons are suggested below, and there may be others:

1) The radiometers themselves, and, therefore, the vertical weighting functions, are not identical. The channels MSU 3 (54.96 GHz) and SSM/T 4 (54.90 GHz) are chosen because they are the most sensitive to temperature at 200-300 hPa where tropical cyclone warm anomalies are strongest. Fig. 3 compares their weighting functions for the two channels based on a tropical sounding and shows that MSU-3 responds to temperatures at slightly lower altitudes. This suggests two opposing influences on tropical cyclone warm anomaly strengths. Less of the stratosphere is observed, and this should result in increased warm anomaly signatures because of the cold pool believed to exist above most tropical cyclones (Koteswaram 1967). But the channel is also more sensitive to conditions below the melting layer, and therefore to reductions in upwelling radiance due to scattering by liquid and wet ice precipitation.

2) The SSM/T limb correction may not be the best for tropical use. Inspection of the data has shown several irregularities, the most frequent of which is limb data (outer element) that are too cold. The data selection routine checks each sector for limb data that differ substantially from

8

Table 2. Summary of results of match pair tests.

	Raw		Retrieved	
	SSM/T	MSU	SSM/T	MSU
minimum	-0.23	-0.47	3.36	1.99
maximum	3.29	2.74	13.38	10.01
range	3.52	3.21	10.02	8.02
mean	1.17	1.02	6.22	4.74
median	0.98	0.94	6.01	4.43
standard. deviation	0.77	0.78	2.04	1.77
Linear fit parameters				
%variance	47		69	
slope:				
regression	0.69		0.72	
maximum likelihood	1.01		0.84	

the rest of the sector and excludes these if found. It is possible that similar, but smaller effects are occurring in other elements resulting in a slight cold bias towards the edges of the sectors. This would tend to lead to a slight amplification of the warm anomalies. Experiments to date have shown that the results are quite insensitive to the choice of 'wet' or 'dry' atmosphere limb corrections.

Though probably due to the raw data and not the retrieval algorithm itself, a systematic difference exists between MSU-based and SSM/T-based retrievals of warm anomaly strength. Before comparing them to each other or using them in other statistical relationships to estimate tropical cyclone intensity, the SSM/T estimates should be corrected using one of the following relationships. Correction of SSM/T rather than MSU does not imply that MSU estimates are more accurate, but is done for convenience because the warm anomaly vs. intensity relationships based on aircraft data are all derived from MSU (Section 2.6).

Linear regression (minimum variance) $dB_{MSU} = 0.259 + 0.719 * dB_{SSM/T}$

$$(2)$$

Maximum likelihood $dB_{MSU} = -0.489 + 0.839 * dB_{SSM/T}$

Because the variances of both SSM/T and MSU warm anomalies are similar, the maximum likelihood solution is preferred. A 10° anomaly retrieved from SSM/T is comparable to a 7.9° anomaly from MSU.

The following items are suggested areas of future research:

1) The weighting functions of MSU-3 and SSM/T-4 for various profiles of temperature and humidity, and the sensitivity of each to cloud and precipitation-sized condensate, both ice and water, should therefore be carried out. The cooler warm anomalies in MSU-3 may be explained by a greater sensitivity to scattering.

2) The current limb correction coefficients and how they were derived should be investigated thoroughly. The limb-corrected data themselves should be systematically evaluated for evidence of any systematic limb-to-center bias in the tropics.
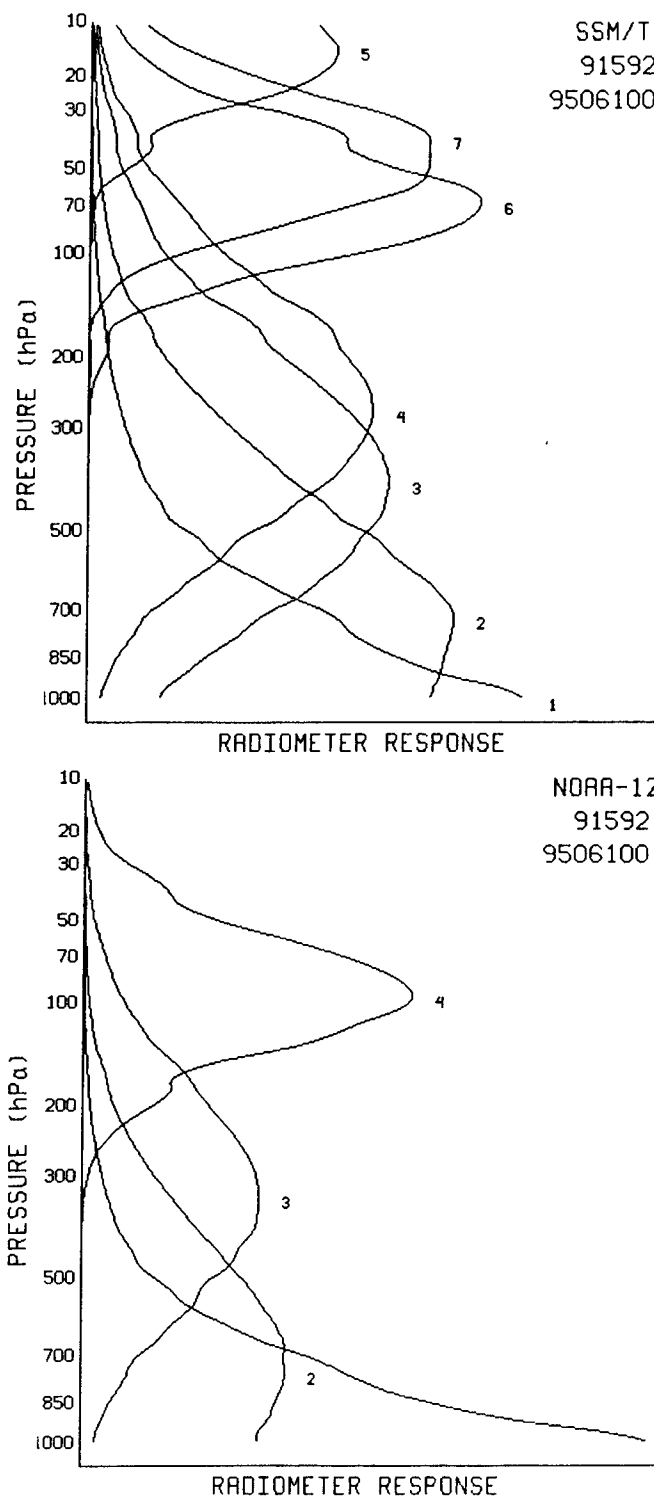
Fig. 3. Weighting functions for SSM/T (top) and MSU (bottom) computed for a tropical sounding.

3) This match pair study itself has some possible limitations which should be addressed in the future. The eye radii were all estimated using infrared window channel satellite imagery, either from AVHRR or a geostationary satellite, and these are now known to be inferior to eye radius estimates from SSM/I, especially for less intense deepening and most filling storms where the eye is partially obscured by cirrus (see Section 2.7). The eye radii may be underestimated in these cases, and depending upon viewing geometry this can affect SSM/T and MSU retrievals differently (Merrill 1995). The match pair experiment should be repeated using SSM/I data for eye size estimates. Availability of SSM/I data should also allow stratification of the match pair set by core rain rate or an approximation thereof, allowing a test of the hypothesis that the stronger raw warm anomalies in SSM/T are due to the smaller effects of scattering by precipitation.

2) Raw brightness temperatures, especially from lower tropospheric channels that are especially sensitive to precipitation, should also be compared. Analysis of historical MSU history data indicates that channel 2 is inversely correlated with warm anomaly strength (see Section 2.10 "Possible Rainfall Effects") and can be used to correct the warm anomaly *vs.* intensity relationship for MSU. A similar corrector should be sought for SSM/T, with channel 2 suggested as a starting point.

2.6.   Retrieved Warm Anomaly Strength as an Estimator of Typhoon Intensity

The horizontal physical retrieval algorithm, plus the statistical relationships described in Section 2.5, allow production of estimates of interchangeable estimates of upper-tropospheric warm anomaly strength from both SSM/T and MSU. As described in Section 2.2, such an estimate alone is still insufficient for direct calculation of intensity (maximum sustained wind or minimum sea level pressure), so a statistical relationship fitting retrieved warm anomaly strengths to *in situ* intensity measurements must still be used. Such a relationship can be obtained by running the horizontal structure retrieval on the Velden *et al.* (1991) data set and redoing the statistical analysis described in Section 2.3.

The relationship between sea level pressure reduction and raw and retrieved warm anomaly strengths are shown in Figs. 4 and 5, respectively. Problems with data format conversion caused three cases to be lost, leaving a total of 79. Of those, 53 had an eye size reported by the aircraft and therefore available for a constraint for the horizontal structure retrieval. In the remainder of the cases, an estimated mean warm anomaly radius of 24 km was used. The following regression relationship is obtained.

$$dP = -9.53 + 9.95*dB_{ret} - 0.25*(dB_{ret})^2, \; SEE = 17.8 \; hPa \tag{3}$$

The results are qualitatively similar to those reported in Velden *et al.* (1991) but are disappointing in several respects:

1) The warm anomaly strength from the horizontal structure retrieval algorithm is a much poorer estimator of pressure reduction than is the 250 hPa temperature anomaly calculated from vertical soundings with no horizontal retrieval (see Section 2.3). The standard errors of estimate are 17.8 hPa and 13.7 hPa, respectively. The difference of three cases in the sample size is not believed to contribute significantly.
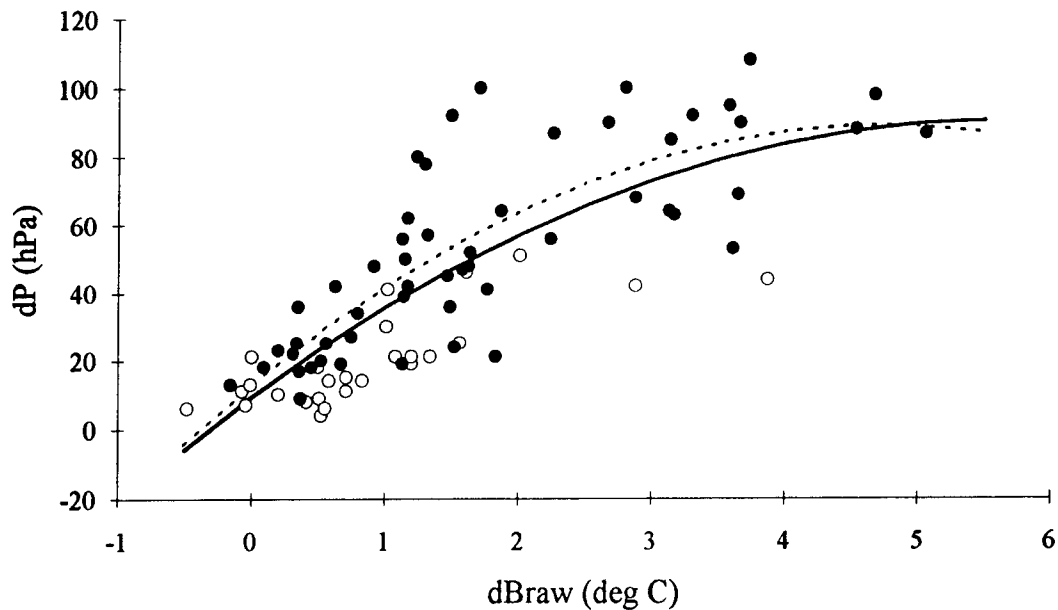
Fig. 4. Relationship between sea level pressure reduction (environmental pressure minus MSLP reported by reconnaissance aircraft) and raw warm anomaly strength, computed as described in Section 2.5. Crosses denote cases for which the aircraft did not report an eye diameter. Two quadratic least squares fits are shown. The solid curve is a fit to the entire data set, whether an eye was reported or not. It explains 64.6% of the variance in dP and has a standard error of estimate of 17.3 hPa. The dashed curve was fitted only to the 53 cases for which an eye was reported. It explains 35.1% of the variance with SEE of 22.9 hPa.

2) Retrieved warm anomaly strengths from the horizontal structure retrieval algorithm are poorer estimators of intensity (pressure reduction) than warm anomalies computed directly from raw brightness temperatures for the entire 79 case sample. The percentages of variance explained are 62.9% and 64.6%, respectively.

The negative result 2) is believed to be due in part to the quality of eye size estimates. If only the 53 storms having reported eyes are considered, the retrieved warm anomalies are superior to the raw ones, and quadratic least squares curves explain 44.3% and 35.1% of the variance in dP, respectively. The retrieval algorithm is making a positive contribution when an actual, rather than mean, eye size is made available. This is consistent with the findings of Merrill (1995) that a good *a priori* estimate of warm anomaly size is critical. The reduction of variance is lower and SEE higher than for the 79-case sample because many of the storms with no reported eye were weaker. When these were eliminated, the average intensity (and variance) of the sample goes up, making the problem of estimating dP 'harder.'

The following items are suggested areas of future research:

1) The eye size estimates used in the 79 cases should be reviewed using other data sources, including archived satellite imagery and radar reports. If possible, the aircraft reports themselves should also be re-examined. Many intense storms are now known to have 'concentric' eyes, and it is thought (though not proven) that the outer eye radius is more representative of the warm
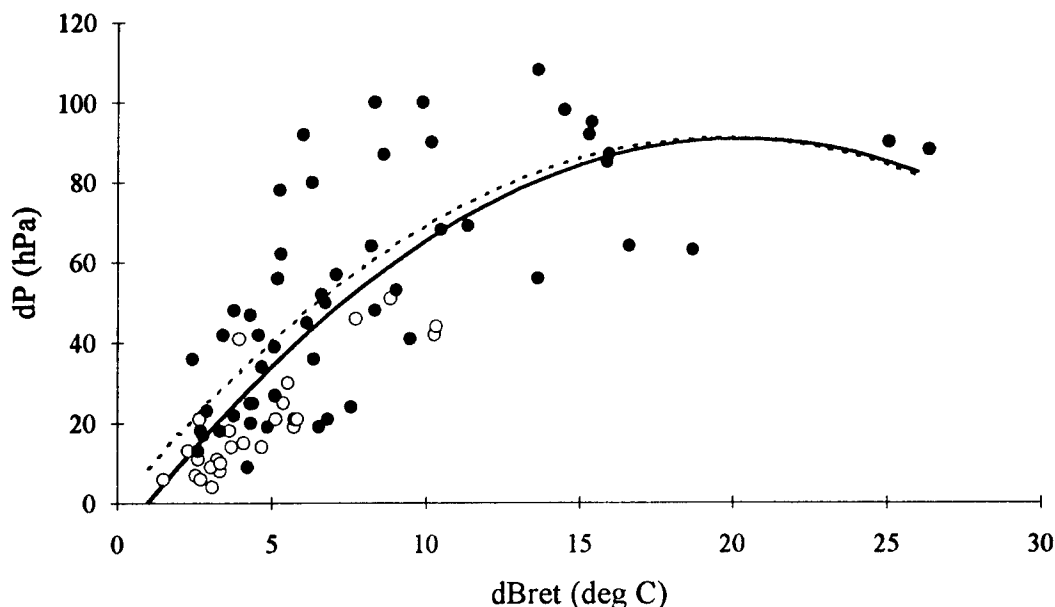
Fig. 5. Same as Fig. 4 but for retrieved warm anomaly strengths. The quadratic least squares fit to all cases explains 62.9 % of the variance with SEE of 17.8. For cases with reported eyes, the fit results are 44.3% and 21.3 hPa.

anomaly horizontal scale. It might also be possible to assign actual eye radii to some of the cases with no aircraft eye size based on satellite or land-based radar.

2) The warm anomaly size estimates (constraints) based on aircraft reports of eye size should be altered to reflect the systematic difference between aircraft- and satellite-derived eye size estimates. This should make any statistical relationships based on these data more appropriate for operational use, in which nearly all eye size estimates will be coming from satellites.

3) The brightness temperature data themselves should be systematically reviewed for bad data points. This might be done using the /d option with XTCR to dump the channel 3 MSU brightness temperatures into a file, from which they can be inspected using a contour-analysis package or a commercial spread sheet package.

4) After the above changes have been made, the retrievals should be rerun and the statistical relationships rederived. They will be an important component of the operational use of retrieved warm anomaly strengths.

Another factor is the effect of scattering due to precipitation. In an experiment described in Section 2.10 topic "Possible Rainfall Effects," using the raw channel 2 brightness temperature nearest the storm center (B_2) as an intensity estimator along with the retrieved warm anomaly strength yields the following relationship

$$dP = -24.50 + 12.07*dB_{ret} - 0.30*(dB_{ret})^2, - 4.33*(B_2-260°K), \quad SEE = 15.4 \text{ hPa} \tag{4}$$

13

which, though still inferior to that of Velden *et al.* (1991) based on 250 hPa temperatures, is an improvement over (3). Because of antenna pattern and spectral differences, MSU B_2 and SSM/T B_2 are probably not interchangeable so (4) cannot be used in a two-satellite operational method. An equivalent of the B_2 term that is interchangeable between MSU and SSM/T should be sought (see Section 2.5).

2.7. Estimating the Horizontal Scale of the Warm Anomaly: The "Eye Size" Problem

Proposal task: Eliminate dependence on *in situ* observations, specifically warm anomaly horizontal scale as estimated from the eye size.

Simulations show that the horizontal structure retrieval algorithm is very sensitive to biases in the warm anomaly horizontal scale (Merrill 1995). For the data set described in Section 2.5, the radius of the eye, as estimated from infrared window channel satellite imagery, has been used as an estimate of the horizontal scale of the warm anomaly. When an eye is not present, a 'reasonable' value of 20-30 km is used at the operator's discretion. For the 1980-84 data set used in Velden *et al.* (1991) and Section 2.3, the eye radius was that reported by reconnaissance aircraft, presumably based on their airborne radar. It would seem that eye radius is the only practical proxy measurement for operational use, but this raises several issues:

1) Is eye radius an unbiased estimate of the actual warm anomaly scale parameter, or is the actual warm anomaly scale systematically larger or smaller at certain stages in a tropical cyclone's life,

2) How accurately can eye radii be estimated from satellite, and

3) Can regression relationships between warm anomalies retrieved using aircraft eye radii (Section 2.3) be applied to warm anomalies retrieved using satellite eye estimates?

The first question is the most difficult to answer because very few *in situ* observations of warm anomaly radius by high-altitude aircraft are available, and even when they are it is difficult to estimate what the eye radius estimate would have been under the circumstances. As discussed in Merrill (1995), temperature profiles from two Atlantic hurricanes were used to fit the profiles, and the warm anomaly scale used to fit the observed profile was at least reasonably close to the likely eye diameter of the storm. With only two cases, it is impossible to be more precise.

Simultaneous collection of SSM/I data began near the end of the project and data are available for only a few weaker systems, one strong typhoon, and a portion of another so it is impossible to draw any quantitative conclusions. But qualitatively, the eye size estimates from SSM/I are judged to be quite superior. An example is shown in Fig. 6. As seen by the infrared imager (AVHRR), the eye radius is unchanged at about 10 km over the 12 h period of the observations. But the microwave imager (SSM/I) shows the development of an outer concentric eye with a radius of about 60 km. It is unfortunately very difficult to draw any clear conclusions about which eye radius (inner or outer) is 'better' in this case because the raw warm anomaly strengths also vary unexpectedly (Table 3) in the manner described in Section 2.5. In the first pair, the MSU raw warm anomaly is stronger, as would be expected because of the smaller antenna pattern, and the horizontal retrieval algorithm produces nearly identical estimates of the warm anomaly strength. But in the second pair, the MSU warm anomaly is nearly unchanged while the SSM/T raw warm anomaly has more than doubled. Regardless of the choice of eye size, the retrieved warm anomaly from SSM/T is much larger than that from MSU. If we consider the effect of eye size on the second MSU estimate, we see that use of the small eye in Fig. 6c yields a warm anomaly strength almost identical to that of the first MSU estimate, and use of the large eye produces a substantial weakening. The rationale for the averages, either linear or RMS (the radius of an 'eye' having the average of the areas of the large and small eye), is that the warm anomaly is probably spreading out gradually as
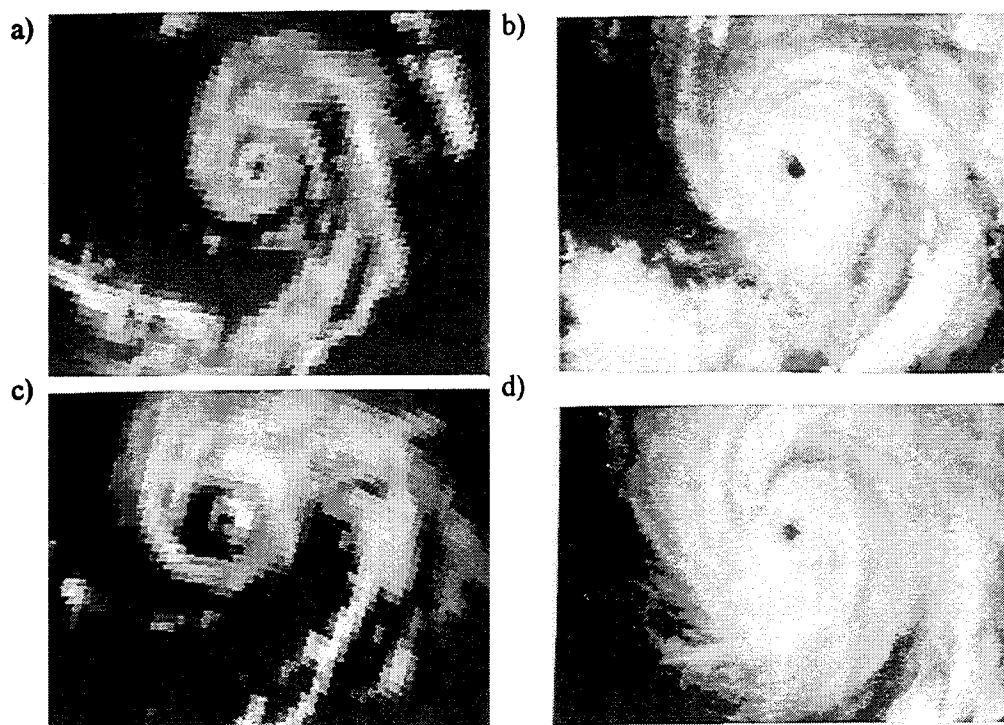
Fig. 6. Nearly simultaneous pairs of SSM/I (left) and AVHRR (right) images of Typhoon "Walt" (July 1994). a) DMSP-10 SSM/I Band 6, 21:18 UTC 19 July, b) NOAA-12 AVHRR Band 4, 22:24 UTC 19 July, c) as (a) but 9:37 UTC 20 July, and d) as (b) but 8:34 UTC 20 July.

Table 3. Raw and retrieved warm anomaly estimates for the Typhoon Walt cases for which imagery is shown in Fig. 6.

Time	Satellite	R(eye)	dB(raw)	dB(ret) small	R(eye) average	dB(raw) RMS	dB(ret) large
21:18	DMSP	10	1.2	8.9	8.9	8.9	8.9
22:24	NOAA	10	1.5	8.7	8.7	8.7	8.7
8:34	DMSP	11 / 62	3.1	13.7	11.6	8.2	7.4
9:37	NOAA	11 / 62	1.6	9.0	7.9	5.7	5.0

the inner eye wall convection collapses. It is unfortunate that there are no *in situ* measurements of central pressure for cases like this.

The answer to the third question depends upon the relationship between aircraft and satellite eye estimates. An unpublished study and data set by Thorson and Zehr (1994) indicates that the aircraft eyes are slightly larger, but with considerable scatter. As has been noted, the accuracy of a satellite eye size estimate depends strongly on the type of sensor, with SSM/I estimates believed to be far superior to those from visible or infrared sensors in some cases. The satellite eye reports come from the 'remarks' section in fix messages, and the majority of the fixes probably came from infrared rather than SSM/I, although this is not known. It is tentatively concluded that, relative to the other sources of error, discrepancies between aircraft and satellite eye estimates are of secondary importance. The exceptions may be in those cases where the storm had a concentric eye and the aircraft report used in Section 2.3 mentioned only the inner eye radius when the outer radius would have been more appropriate.

2.8. Operational Potential

Proposal task: Evaluate the operational potential of MSU and SSM/T for tropical cyclone monitoring.

See Sections 2.5-2.7.

2.9. Transfer to Operations

Proposal task: Assist in the transfer of the results to operations via a scientific and technical description of the algorithm, the source code, and documentation.

A list of "where to find it" follows.

2.9.1 Scientific Description of Algorithm

Refer to Merrill (1995), Chapter 2 Sections 2.2 and 2.5-2.7 and the Users' Guide (available from the author).

2.9.2 Technical Description of Algorithm

Refer to the Users' Guide and the Software and Development and Maintenance Guide (available from the author).

2.9.3 Source Code

The source code is available from the author on diskettes (2).

For installation and use instructions, refer to Users' Guide.

For description of the internal structure of the software, refer to the Software Development and Maintenance Guide.

2.9.4 Documentation

Self-contained documentation for using the algorithm is found in the Users' Guide (Chapter 3). Persons requiring an in-depth understanding of the algorithm's implementation are referred to the Software Development and Maintenance Guide.

2.9.5 Suggested Input Constraint Values

The present (6/94) values and their origins are described in Merrill (1995). They are also listed in the Users' Guide.

Refer also to the Software Development and Maintenance Guide for a suggested change in how the software handles constraints.

2.9.6 Sample Data Sets

A sample data set is included on the source code diskettes distribution. Refer to the Users' Guide.

2.10. Related Research Areas

Proposal task: Continue research on various topics related to monitoring tropical cyclone intensity using passive microwave observations.

2.10.1 Anomalies in Other Channels

This was not attempted, with the exception of topic "Possible Rainfall Effects" below. In principle, the horizontal retrieval algorithm could be applied to channel 4 of MSU and channel 5 of SSM/T to retrieve the lower stratospheric thermal structure. This was not done for several reasons, all relating to the validity of the assumptions made in deriving the horizontal structure retrieval algorithm:

1) The shape of the warm anomaly, even when non-dimensionalized by the amplitude, probably varies significantly with height over the depth of these weighting functions because they straddle the tropopause. The tropopause topography and thermal characteristics over tropical cyclones are generally unknown.

2) No *in situ* information about the horizontal structure of the lower stratospheric thermal anomaly is available so suitable constraints and estimated error covariances would be difficult to specify.

One possible way to make better use of the stratospheric information is via an 'upper tropospheric retrieval' using the upper tropospheric and lower stratospheric microwave channels in conjunction with infrared sounding channels (HIRS). The HIRS channels may be able to provide detailed soundings of the thermal structure above the cloud shield with a horizontal resolution of about 25 km, and this information could then be combined with the microwave channels to make a sounding of that portion of the atmosphere above the melting level. This would represent a partial solution to the sounding problem described in Section 2.2.

2.10.2 Optimal Vertical Level for Computing delT from Soundings

This was not attempted.

2.10.3 Possible Rainfall Effects

Velden *et al.* (1991) noted that warm anomalies computed from 250 hPa temperatures retrieved from all four MSU channels were a better predictor than warm anomalies computed from channel 3 brightness temperatures alone. It is believed that the sounding retrieval used to produce the 250 hPa temperatures is able to use the lower-tropospheric channels (1 and 2) to compensate partly for the slight cooling of channel 3 due to scattering by precipitation.

Preliminary research using the MSU 'history' data set (see Section 2.6) indicates that channel 2 data can also be used to improve intensity estimates from retrieved warm anomaly strengths based on upper-tropospheric data (channel 3 MSU or channel 4 SSM/T). The 'brief' (.TXT) output (see Users' Guide) contains the limb-corrected channel 2 brightness temperature (B_2) for the field of view nearest the storm center. When included in the regression relationship between storm intensity and warm anomaly strength, the standard error of estimate is reduced from 17.8 to 15.4 hPa and the reduction of variance increases from 62% to 72%. Channel 1 was also considered and provides much less additional information than B_2. The channel 2 signal is believed to be strongly influenced by precipitation because the mean B_2 value is about -14°C. The weighting function for channel 2 peaks at 600-700 hPa where air temperatures are typically 0-10 °C in the undisturbed tropics and perhaps 5 °C warmer in tropical cyclones (10-20 °C

warmer in the eye). The coefficient on B_2 is negative, indicating that the colder the B_2, the greater the intensity for a given warm anomaly strength.

This is an encouraging, though incomplete, result. First, it is not quantitatively interchangeable between SSM/T and MSU. A similar phenomenon is probably occurring in both because the warm anomaly strength estimates are similar (see Section 2.5) and this would not be the case if scattering by precipitation were a significant influence on the upper-tropospheric channel for one sensor but not another. Second, using B_2 as a linear corrector is probably a less than optimal use of the available data to correct the upper tropospheric warm anomaly strengths for scattering. A better solution would be to retrieve the three-dimensional structure of precipitation using all available data (especially SSM/I) and use the hydrometeor distribution, the MSU or SSM/T antenna pattern, and the upper-tropospheric weighting functions to predict the influence of precipitation on the upper-tropospheric channels and remove it prior to running the horizontal structure retrieval.

Another possibility is that the relationship between B_2 and intensity may be somewhat indirect and not all directly attributable to scattering. Velden *et al.* (1991) notes that deepening storms typically have a much weaker warm anomaly than filling storms of the same intensity, even when 250 hPa temperatures from a sounding retrieval algorithm are used to compute the warm anomaly. Since precipitation effects are accounted for at least in part by the sounding retrieval, it is believed that the difference between deepening and filling storms must be due to other factors as well. One of these is the upward shift in the location of the warm anomaly, especially in the eye, as storms begin to fill (Jordan 1961). The higher the warming, the more evident it is in upper-tropospheric channels and, all things being equal, the stronger the retrieved warm anomaly. Other investigators (Zehr 1987) have shown that rainfall rates are typically larger in deepening storms than in filling ones. A similar relationship is evident for B_2; the coldest B_2 values (and by implication heaviest precipitation) are found with deepening storms, typically when the rate of central pressure fall over the most recent 12 h is greater than the fall over the 12 h period ending 12 h ago.

2.10.4 Eye Sounding Feasibility Study

Evidently the sounding retrieval algorithm on McIDAS was able to make use of the information in the other channels in a constructive fashion despite scattering due to precipitation. A simple attempt was made in the second quarter of 1990 to make a better eye sounding by using the results of the horizontal retrieval in place of the MSU 3 raw brightness temperature as input to the sounding retrieval. The experiment was conducted for Typhoon "Orchid" of 1993 and ended in failure. The retrieved sounding showed excessive warming in the upper troposphere and unrealistic cooling of up to 25 °K between the surface and 350 hPa. Future experiments in this direction will require a detailed knowledge of the sounding retrieval algorithm and the ability to modify its constraints and input error checking (if that exists) to accommodate the extreme MSU-3 values produced by the horizontal retrieval. A satisfactory solution may not even be possible without a consistent horizontal retrieval algorithm for the other channels besides channel 3, which in turn requires a means of accounting for scattering effects.

3. Users' Guide Overview

The software referred to in this report is a working prototype of an algorithm to retrieve the horizontal structure of the upper tropospheric warm anomalies of tropical cyclones from passive microwave data. The prototype implementation of the horizontal structure retrieval algorithm consists of two programs — XTCR (eXperimental Tropical Cyclone Retrieval) and XTCRLOG (eXperimental Tropical Cyclone Retrieval LOG) and several types of data file. The source code and data files are available from the author. The whole system is referred to as the 'XTCR package' in the Users' Guide. The term 'prototype' is chosen consciously. Even 'casual' users of the system with the demonstration data set must have at least a basic familiarity with DOS and be able to use the basic DOS file system commands (CD, TYPE, etc.). Real-data use with an existing installation will require access to tropical cyclone and satellite information. Installing the system requires at minimum access to, and ability to configure and use properly, Microsoft FORTRAN version 5.1 and Microsoft C version 6.0 compilers. The code will require modification for use in other environments.

The Users' Guide is intended for users of the prototype package after it has already been set up and for software professionals who will be setting up the package. Software professionals needing to understand the inner workings of the package to resolve bugs or modify it should refer to the Software Development and Maintenance Guide as well as the Users' Guide. The complete versions of these two guides are available from the author.

4. Software Development and Maintenance Guide Overview

The following is a brief description of the Software Development and Maintenance Guide which is available from the author. This Guide is addressed to those wishing to understand the internal structure of the XTCR package with a view to adapting it to new environments or modifying it. It assumes a knowledge of FORTRAN and C syntax and general programming practices. It is also assumed that the environment in which you are working has a source code database utility such as PWBRMAKE of the Microsoft Programmers' Workbench (PWB) to answer questions like 'where is variable X defined' and 'what is the calling sequence for routine F.' This Guide concentrates on design, algorithms, data structures, and 'helpful hints' that are not really accessible using a source browser.

The XTCR package has been under development for about 5 years. In its earliest form, it could only use historical MSU data sets in a now-obsolete format and retrieved only six structure variables rather than the present eight (Merrill 1991). The code was then generalized to allow retrievals using simulated data, and warm anomaly latitude and longitude were added to the list of retrieved variables so the effects of errors in real-time position estimates could be evaluated. This version was used to support the research described in Merrill (1995) and, like earlier versions, was written entirely in Microsoft FORTRAN, though not ANSI-conforming due to dynamic memory allocation and calls to the Microsoft C graphics library.

5. Publications and Presentations Supported by this Project

5.1 Refereed Publications

Velden, C. S., B. M. Goodman, and R. T. Merrill (1991): Western North Pacific tropical cyclone intensity estimation from NOAA polar-orbiting satellite microwave data. *Mon. Wea. Rev.*, 119, 159-168.

Merrill, R. T. (1995): Simulations of physical retrieval of tropical cyclone structure using 55 GHz band passive microwave observations from polar-orbiting satellites. *J. Appl. Meteor.* 34, 773-787.

5.2 Conference Presentations

Merrill, R. T. (1991): Physical retrieval of typhoon structure using passive microwave observations. *19th AMS Conf. on Hurricanes and Tropical Meteor.*, 6-10 May, Miami, FL. 405-408.

Velden, C. S. and R. T. Merrill (1990): Western North Pacific tropical cyclone intensity estimation from NOAA polar orbiting satellite microwave data. *5th Conf. on Satell. Meteor. and Ocean.*, AMS/RMS, London, 3-7 Sep.

6. References

Craig, J. C. (1990): *The Microsoft Quick C Programmer's Toolbox.* Microsoft Press, Redmond, WA. 525 pp.

Dvorak, V. F. (1975): Tropical cyclone intensity analysis and forecasting from satellite imagery. *Mon. Wea. Rev.*, 103, 420-430.

Dvorak, V. F. (1984): Tropical cyclone intensity analysis using satellite data. *NOAA Tech. Report NESDIS 11*, 47 pp.

Jordan, C. L. (1961): Marked changes in the characteristics of the eye of intense typhoons between the deepening and filling stages. *J. Meteor.*, 15, 779-789.

Koteswaram, P. (1967): On the structure of hurricanes in the upper troposphere and lower stratosphere. *Mon. Wea. Rev.*, 95, 541-564.

Merrill, R. T. (1995): Simulations of physical retrieval of tropical cyclone structure using 55 GHz band passive microwave observations from polar-orbiting satellites. Accepted for publication by *J. Appl. Meteor.*

Prata, A. J., M. J. Lynch, R. Hille, and L. van Burgel (1986): Observations of tropical cyclones in Western Australia using combined TOVS and AVHRR radiances. *Tech. Proc. of 3rd Intl. TOVS Study Conf, Madison, WI, 13-19 Aug.*, 222-234.

Velden, C. S. (1989): Observational analysis of North Atlantic tropical cyclones from NOAA polar-orbiting satellite microwave data. *J. Appl. Meteor.*, 28, 59-70.

Velden, C. S., B. M. Goodman, and R. T. Merrill (1991): Western North Pacific tropical cyclone intensity estimation from NOAA polar-orbiting satellite microwave data. *Mon. Wea. Rev.*, 119, 159-168.

Velden, C. S. and W. L. Smith (1983): Monitoring tropical cyclone evolution with NOAA satellite microwave observations. *J. Clim. Appl. Meteor.*, 22, 714-724.

Zehr, R. A. (1987): The diurnal variation of deep convective clouds and cirrus with tropical cyclones. *17th AMS Conf. on Hurr. and Tropical Meteor., Miami, FL, 7-10 April*, 276-279.

Zehr, R. A. and W. Thorson (1994): Personal communication.